ACS APPLIED MATERIALS & INTERFACES

Research Article

www.acsami.org

Glutaraldehyde Vapor Cross-linked Nanofibrous PVA Mat with in Situ Formed Silver Nanoparticles

Addisu Getachew Destaye, Cheng-Keng Lin, and Cheng-Kang Lee*

Department of Chemical Engineering, National Taiwan University of Science and Technology, No.43, Sec. 4, Keelung Rd., Da'an Dist., Taipei City 106, Taiwan, Republic of China

Supporting Information

ABSTRACT: Polyvinyl alcohol (PVA) nanofibrous mat can be easily prepared via electrospinning its aqueous solution. However, the obtained nanofibrous mat is instantaneously dissolved in water. Therefore, rendering the environmentally friendly nanofibrous mat water insoluble by cross-linking mechanism is of great interest. The electrospun PVA nanofibrous mat with an average fiber diameter of ca. 400 nm could be effectively cross-linked by glutaraldehyde vapor at room temperature. The cross-linking not only resulted in a water-insoluble nanofibrous mat but also generated an excess amount of unreacted aldehyde functional groups that could reduce silver salts into silver nanoparticles. The in situ formed silver nanoparticles along the fibrous surface showed excellent antimicrobial activity against *Escherichia coli*. The vapor cross-linked nanofibrous mat shows a high potential to be used for efficiently capturing and killing pathogenic bacteria.

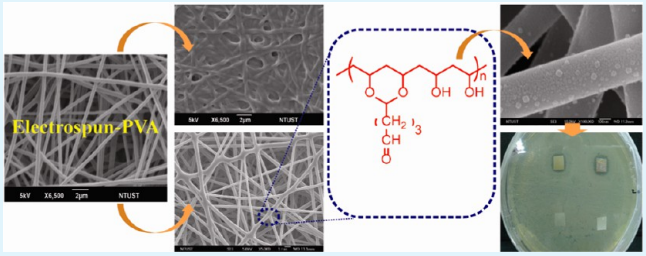

KEYWORDS: *PVA, glutaraldehyde, vapor cross-linking, nanofibrous mat, silver nanoparticles, antibacterial activity, electrospinning*

INTRODUCTION

When the diameters of polymeric fibers are decreased down from micrometers to submicrometers or nanometers, there appear several remarkable characteristics such as extremely large surface area to volume ratio, flexibility in surface functionalities, and superior mechanical performance (e.g., stiffness and tensile strength) compared with any other known form of the material. These outstanding properties make the polymer nanofibers to be optimal candidates for many important applications.[1−5] Electrospinning is a powerful and effective technique that provides a relatively inexpensive method of producing continuous polymeric fibers with nanoscaled diameters through the action of an external electric field imposed on a polymer solution or melt.[6−10] However, successfully electrospun polymeric nanofibers are not easily obtained. In addition to correctly adjusting the electrospinning parameters such as voltage applied and flow rate of polymeric solution employed, usually a suitable solvent for the polymer dope preparation is required for obtaining electrospun nanofibers. Polyvinyl alcohol (PVA) is a hydrophilic, nontoxic, biocompatible, biodegradable synthetic polymer with good chemical, thermal, and mechanical stability and wide range of crystallinity.[1,7,10−14] Recently, PVA has been demonstrated to be easily electrospun into nanofibrous mat from its aqueous solution.[15−20] However, the obtained electrospun PVA nanofibrous mat when immersed in water instantaneously dissolves and becomes a clear gelatinous like material,[9,21,22] which limits its applications in wet state. For most applications, therefore, rendering the environmental friendly nanofibrous mat water insoluble by either cross-linking or grafting hydrophobic segments to the PVA hydroxyl groups is of paramount importance.[9,10,21−24] PVA can be cross-linked using physical methods such as heat and radiation or chemical agents including but not limited to glutaraldehyde, glyoxal, and boric acid.[9] Glutaraldehyde (GA) is a more effective cross-linking agent than other aldehydes[25] and one of its approach that has been investigated is its vapor phase exposure to nanofibrous mats because it has less or no cytotoxic effect.[10,23,26,27]

In recent years, immobilization of metal nanoparticles onto electrospun polymeric nanofibers, because of the nanofibers possessing flexibility, high surface area, high porosity, and good mechanical strength,[10] has been researched for applications such as bio/gas sensing,[10,28] catalysis,[29] sensitive substrates for SERS,[30,31] antimicrobial wound dressing,[32] and in environmental applications,[33] to mention a few among other applications. Metallic nanoparticles and their corresponding metallic oxides, for instance, copper,[34] gold, silver,[35] and ZnO,[36,37] CuO, TiO_2[37] have received considerable attention due to their outstanding physical, chemical, and biological properties and potentials in several applications. Among them, silver nanoparticles have been investigated most intensively because they have the advantage of a very broad spectrum of antimicrobial activity and relatively low toxicity to humans.[38−41] Metal nanoparticles, when they are in solution, have a tendency to form aggregates in order to minimize their surface energy. However, the aggregation of Ag nanoparticles diminishes their

Received: December 31, 2012
Accepted: May 13, 2013
Published: May 13, 2013

   dx.doi.org/10.1021/am401730x | ACS Appl. Mater. Interfaces 2013, 5, 4745−4752

Scheme 1. Schematic Illustration of (a) the Reaction of PVA with GA and its Intermolecular and/or Intramolecular Cross-Linking Product and the Unreacted End of the Aldehyde, (b) Reduction of Silver Ions by the Unreacted End of Aldehyde in the GA Vapor Cross-linked PVA Nanofibrous Mat

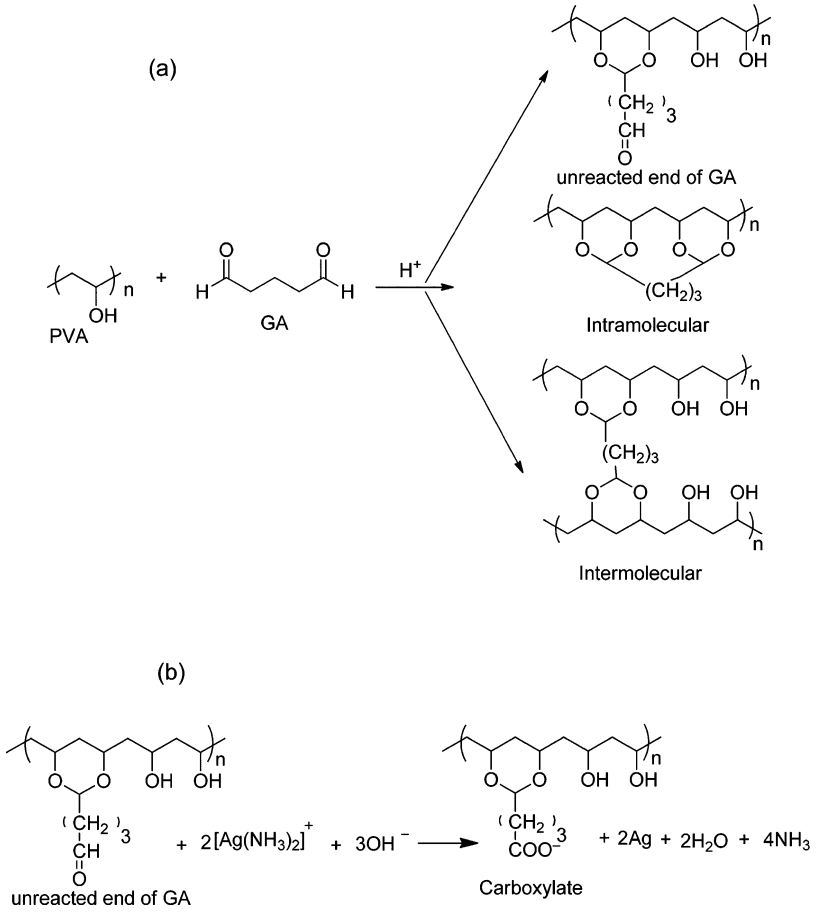

antimicrobial activity.[39−41] To overcome this drawback, Ag nanoparticles can be formed and immobilized onto polymeric matrices, for example, nanofibers that provide high surface area to volume ratio, high porosity, and flexibility.[32,39−42]

In this work, we aim to prepare a PVA nanofibrous mat via electrospinning method and cross-link it with GA vapor at room temperature as a novel technique to obtain a water insoluble nanofibrous mat with in situ formed and immobilized silver nanoparticles. The cross-linking reaction is due to the formation of acetal bridges between the hydroxyl groups in PVA and the difunctional aldehyde molecule of GA.[9] These cross-linking reactions between PVA and GA can be intramolecular and/or intermolecular cross-links[23,24] and this vapor cross-linked PVA nanofibrous mat also found to contain unreacted aldehyde end[14,43] (Scheme 1). Hong et al.[44] reported that electrospun PVA/silver nitrate was reduced to silver nanoparticles by using heat and UV irradiation. However, in this work, the unreacted end of GA in the cross-linked PVA nanofibrous mat was used to reduce silver ion into silver nanoparticles at room temperature. Neither additional reducing agents nor any toxic reagents were employed for Ag nanoparticles generation. *Escherichia coli* was used as a model microorganism to study the antimicrobial activity of the as-prepared PVA nanofibrous mat.

EXPERIMENTAL SECTION

Materials. Polyvinyl alcohol (PVA, degree of polymerization, 2000; M_w = 81 000−96 000; hydrolysis 98.5−99.4%, Hanawa Chemical Pure, Osaka, Japan), glutaraldehyde (GA, 25% aqueous solution, Alfa Aesar, England), hydrochloric acid (HCl, 37% reagent grade, Scharlau), silver nitrate ($AgNO_3$, 99.8%), sodium hydroxide (NaOH, laboratory grade, Fisher Scientific), sodium borohydride ($NaBH_4$, 98% ACROS-Organics), sodium cyanoborohydride ($NaCBH_3$, 95% ACROS-Organics), sodium carbonate anhydride (Na_2CO_3, ACROS-Organics), bicinchoninic acid solution, Sigma), copper(II) sulfate pentahydrate ($CuSO_4{\cdot}5H_2O$, ACROS), tyramine hydrochloride (99%, ACROS-Organics), and ammonia solution (NH_4OH, 35%, analytical reagent grade, Fisher Chemicals) were used without any further purification. All aqueous solutions were prepared with deionized water from EASYpure II LF ultrapure water system.

Electrospinning of PVA. Ten percent PVA solution was prepared by dissolving PVA powder in deionized water at 80 °C with vigorous stirring for 4 h. After the solution was cooled down to room temperature and the pH of the solution was adjusted to 3 with aqueous solution of HCl. The acidified aqueous PVA solution was poured into a 5 mL syringe fitted with 21G blunt end stainless steel needle with 0.5 mm inner diameter. Electrospinning of the PVA solution was carried out in a Nanofiber Electro-Spinning Unit (JYI GOANG ENTERPRISE CO., Ltd.) fitted with high voltage supply (COSMI SC-PME50) by charging the solution at 14.5 kV-17.5 kV and the distance between the needle tip and the collector was set to be 125 mm. The PVA solution was dispensed at a flow rate of 6 μL/min and the electrospun PVA nanofibrous mat was collected onto a PET (polyethylene terephthalate) as a support attached on the grounded stainless steel collector.

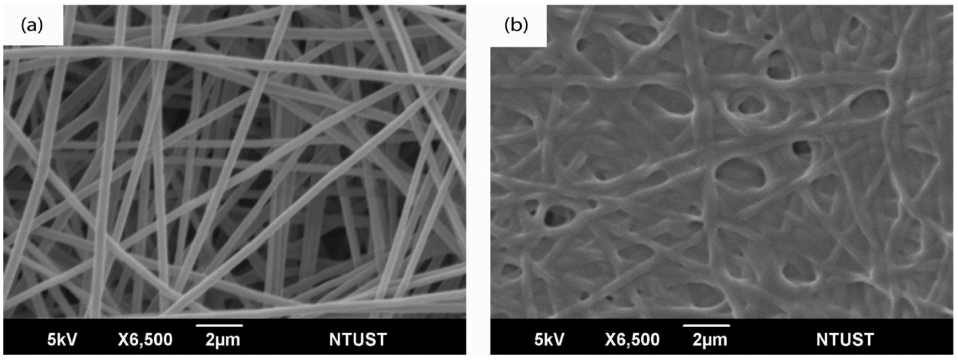

Figure 1. SEM micrograph of (a) as-electrospun PVA nanofibrous mat, and (b) after being soaked/treated in water.

Cross-linking of Electrospun PVA Nanofibrous Mat. As electrospun PVA nanofibrous mat can be dissolved instantly in water, cross-linking of the electrospun nanofibrous mat must be performed before any applications. The cross-linking procedure was carried out with GA vapor in a sealed vessel. Four different concentrations of GA solution were prepared (0.5, 1.0, 2.0, and 2.56 M) and the as-electrospun PVA nanofibrous mat was exposed to the GA vapor for different duration of time (6, 12, 24, and 48 h) for each concentration.

In Situ Generation of Silver Nanoparticles. The in situ reduction of silver (Ag) ion by the unreacted end of the GA in the cross-linked fibrous mat was achieved by immersing the cross-linked PVA nanofibrous mat in 25 mM aqueous silver nitrate ($AgNO_3$) solution overnight at room temperature. Over the course of time, a gradual change of color from white PVA fibrous mat to grayish color was observed. Reducing silver ion by the aldehyde was also carried out by immersing cross-linked PVA nanofibrous mat in 0.1 M ammoniacal silver nitrate solution (Tollen's reagent)[30] for 20 min: briefly, to 10 mL of 0.1 M aqueous $AgNO_3$ was added drops of concentrated ammonia solution while stirring until the brown precipitate, which initially formed, dissolved and became clear solution. To this was added 5 mL of 0.8 M NaOH and the formed precipitate was again dissolved by drops of ammonia solution. The cross-linked PVA mat was then immersed in to the solution and continually swirled for about 20 min. After thoroughly washing with distilled water, the PVA mat was dried at room temperature.

Characterization. The fiber morphology of cross-linked and as-electrospun PVA nanofibrous mat were sputter coated with platinum and characterized by FE-SEM (JEOL JSM-6500F) equipped with an energy dispersive X-ray (EDX) analysis. The average diameter of the fibers was determined by analyzing the SEM image using ImageJ software. The presence of unreacted aldehyde end on the cross-linked PVA nanofibrous mat was confirmed by FTIR-ATR technique (FTS-3500, Bio-Rad). The content of free aldehyde groups on the cross-linked PVA mat was determined by colorimetric method using Tyramine/BCA assay, using tyramine as a labeling reagent for free aldehyde groups: briefly, 1 mL of 200 mM tyramine hydrochloride solution in 0.1 M sodium phosphate buffer pH 6.5 (PBS) and 50 μL of 1 M $NaCBH_3$ solution in water were added to vials containing cross-linked PVA mats (15 × 25 mm^2) and incubated overnight at room temperature under mild shaking. After the pH was adjusted to 10 by Na_2CO_3 addition, 20 mg of $NaBH_4$ was then added to the vials and incubated 2 h under shaking. The cross-linked PVA mats were washed three times with PBS and 0.25 M sodium carbonate buffer solutions (pH 11) to remove any unreacted reagents. A BCA working solution was prepared by mixing 50 parts of bicinchoninic acid solution and 1 part of 4% aqueous $CuSO_4 \cdot 5H_2O$ just before use. One hundred microliters of 0.25 M Na_2CO_3 buffer (pH 11) and 2 mL of BCA working solution were added to the vials containing washed cross-linked PVA mats. The vials were vortexed and incubated for 1 h at 60 °C. After cooling to room temperature, the absorbance was measured at 562 nm.[45] To confirm the existence of silver nanoparticle on the surface of the nanofibrous mat in addition to FE-SEM and EDX, a Jasco V-670 UV spectrophotometer in absorbance mode was used and optical spectra were recorded. The silver content in the nanofibrous mat was determined by immersing weighted PVA mat samples in 25 mL of 10% HNO_3 for 1 h and the resultant supernatant was analyzed by inductively coupled plasma atomic emission spectroscopy (ICP-AES, JY 2000). The mechanical properties of PVA nanofibrous mat both before and after cross-linking with GA were measured under tensile mode in a universal materials testing machine (Testometric, M500−25AT). For the mechanical testing, the PVA nanofibrous mats were cut into rectangular mats of approximate length 25 mm, width 9 mm, and thickness 0.05 mm with load speed of 5 mm min^{-1}.

Antimicrobial Activity. The antimicrobial activity of the silver containing nanofibrous mat was measured by using *Escherichia coli* bacteria as model strain. Luria−Bertani (LB) agar nutrient medium was used for growing the *E. coli*. All the nanofibrous mats used were sterilized by UV-light before the experiment. The antimicrobial activity was examined by spraying *E. coli* bacterial culture with concentration of OD_{600} = 0.05 onto the nanofibrous mat and then placed onto LB agar plate for 24 h at 37 ° C. Inhibition zone method was also employed to measure the antimicrobial activity of the as-prepared nanofibrous mat. The PVA nanofibrous mats were placed onto LB agar already plated with *E. coli* and the diameter of the clear zone was measured after 24 h incubation.

RESULTS AND DISCUSSION

Vapor Phase Cross-linking Reaction of GA. Electrospinning 10% PVA solution produced nanofibrous mat with average fiber diameter of *ca.*400 nm (see Figure 1a). The obtained as-electrospun nanofibrous mat, however, was found instantaneously dissolving in water as it swell considerably and fibers started to fuse with each other and destroy porous openings of the nanofibrous mat (Figure 1b, also see the Supporting Information, Figure S1, for a digital photo). Maintaining the fiber morphology and interfiber pores of nanofibrous mat is important for applications where a high surface-area-to-volume ratio is considered advantageous.

To have PVA cross-linked by GA, the PVA dope solution was adjusted to pH 3 with aqueous HCl so that the obtained electrospun nanofibrous mat contains the required acid catalyst for the cross-linking reaction. The vapor phase cross-linking was performed by employing four vessels with different concentration of GA (0.5, 1.0, 2.0, and 2.56 M) and each vessel was tightly closed with the as-electrospun PVA nanofibrous mat attached onto the inside of the lid exposed to the GA vapor for 6, 12, 24, and 48 h at ambient temperature. After the designated time for the cross-linking reaction, the nanofibers, which were originally straight, became merged and entangled among each other and formed interfiber bonding/fused mostly at the intersection points presumably because of the vapor of aqueous GA (25%) solution contains water vapor

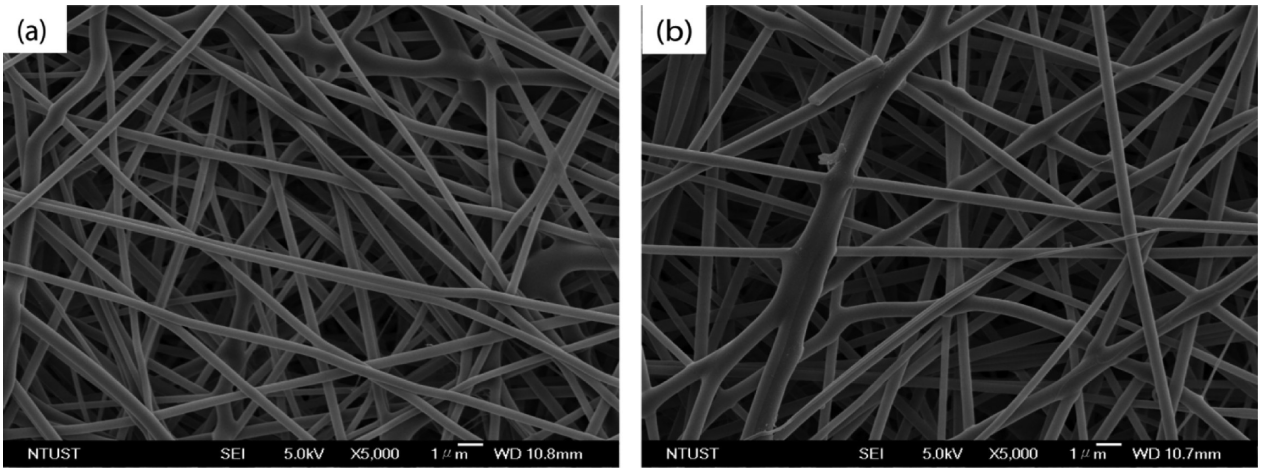

Figure 2. SEM micrographs of vapor phase cross-linked PVA nanofibrous mat with concentration of (a) 2.0 M GA vapor for 48 h, (b) 2.5 M GA vapor for 48 h.

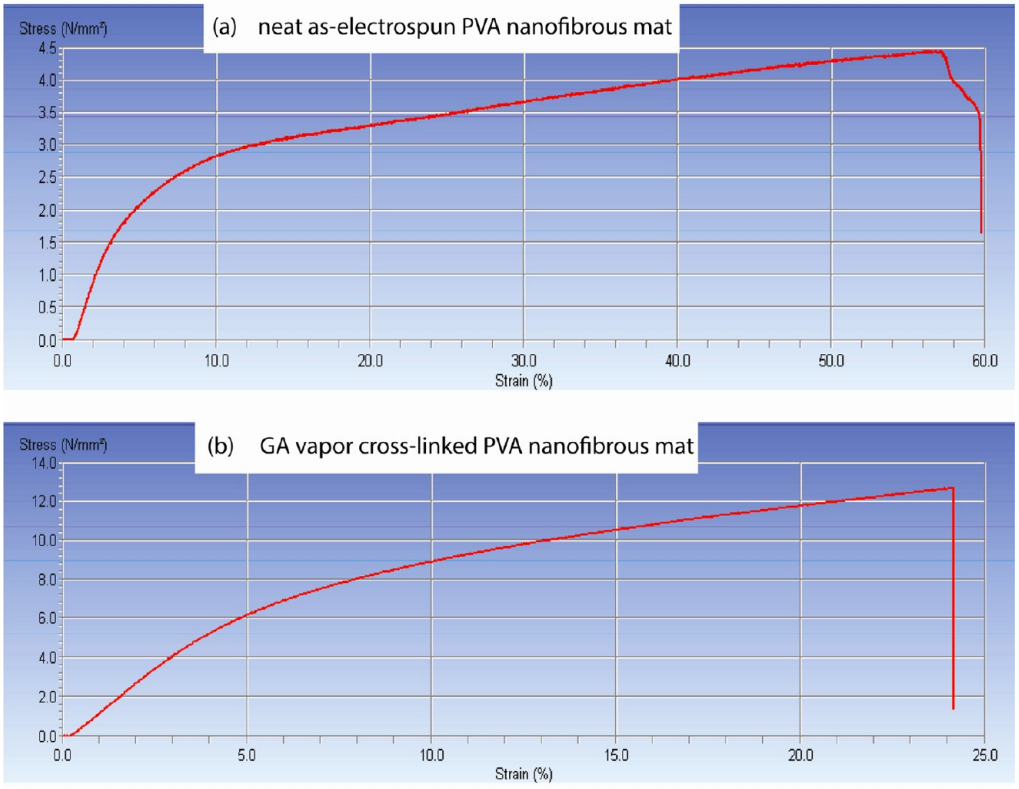

Figure 3. Typical stress–strain curves of (a) neat as-electrospun PVA nanofibrous mat and (b) GA vapor cross-linked PVA nanofibrous mat.

and softening and swelling the surface of the nanofibers leading into contact with nearby nanofibers and intersection points their by form interfiber bonding (see Figure 2a, b). Whereas formation of acetal bridges between the aldehyde ends of the GA and the hydroxyl groups of PVA nanofibers both in intramolecular and/or intermolecular fashion occurred within and at the point of contact between nanofibers. We also observed that with the increase in GA concentration and the cross-linking reaction time, the amount of nanofibers cross-linked increased. With GA concentration increased to 2.0 and 2.56 M, the nanofibers morphology remained unchanged (see the Supporting Information, Figure S2, third and fourth row). Whereas for 0.5 and 1.0 M GA with increased cross-linking time, the nanofibers became swell and flattened (see the Supporting Information, Figure S2, first and second row) because the vapor phase is richer in water than in GA. In other words, the higher water content in vapor phase at lower GA concentration swells PVA nanofibers more effectively than the lower GA vapor concentration can cross-link.

It is noteworthy that for practical applications, the mechanical properties of the electrospun PVA nanofibrous mat are vital. It is known that cross-linking of polymers would improve their mechanical properties.[10,46] Hence, the tensile strength of the neat as-electrospun PVA nanofibrous mat and the GA vapor cross-linked PVA nanofibrous mat were measured to see the effect of cross-linking on enhancing the strength of electrospun PVA nanofibrous mats. Figure 3 showed typical stress–strain curves before (neat PVA) and

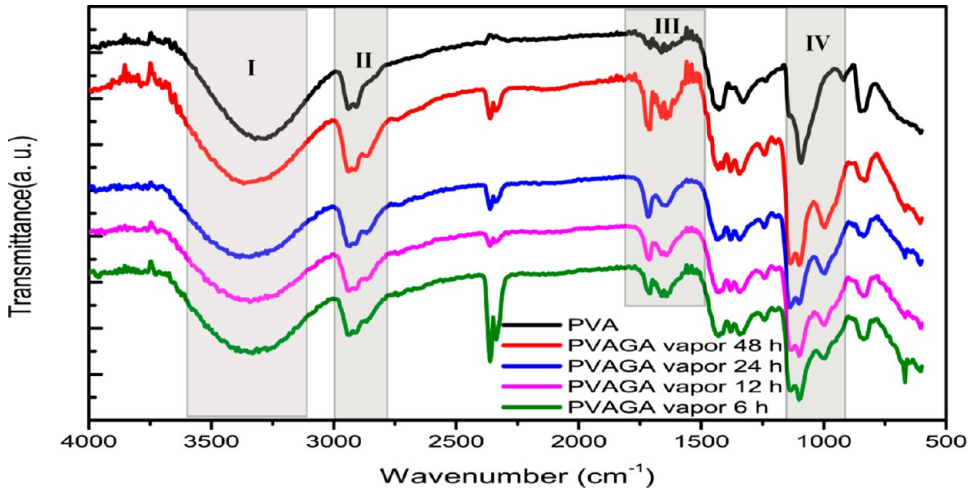

Figure 4. ATR-FTIR spectra of neat electrospun PVA nanofibrous mat and 2.56 M GA vapor cross-linked PVA nanofibrous mat with different vapor exposure time (6, 12, 24, and 48 h) showing the presence of unreacted aldehyde end as exposure time increases and the occurrence of cross-linking.

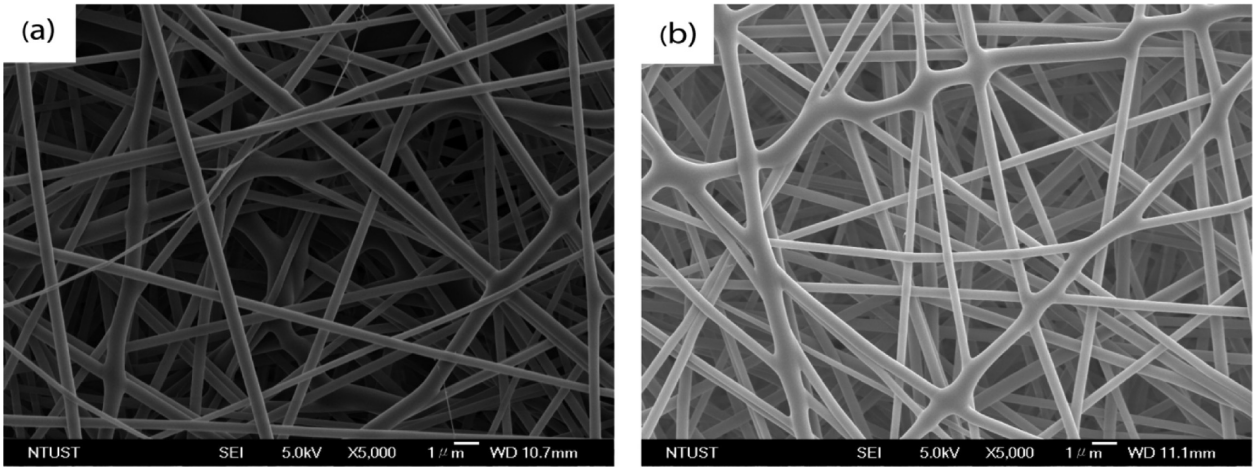

Figure 5. SEM micrographs of (a) vapor phase cross-linked PVA mat, (b) after soaked/treated in water for 48 h.

after (GA vapor) cross-linking. The ultimate tensile strength of the neat as-electrospun PVA nanofibrous mat was measured to be 4.44 MPa and its ultimate strain was 56.19% as shown in Figure 3a. Whereas after GA vapor cross-linking, the ultimate tensile strength of the PVA nanofibrous mat increased about 3 fold to 12.70 MPa and the ultimate strain decreased to 24.14% (Figure 3b). The enhanced ultimate tensile strength indicates that GA cross-linking made PVA nanofibrous mat became mechanically more strong and stable. In addition, the interfiber bonding/fusing of nanofibers occurring mostly at intersection points were also reported to improve the mechanical and physical properties of the cross-linked polymer by providing a rigid web of interfiber bonding.[47]

The presence of unreacted end of the GA on the vapor phase cross-linked nanofibrous mat was confirmed by FTIR. There are four major absorption bands in the spectrum that will change upon cross-linking by GA vapor as shown in Figure 4 for 2.56 M GA vapor exposure (see the Supporting Information, Figure S3 for FTIR spectrum of 0.5, 1.0, and 2.0 M concentrations). The large, broad band observed at 3200−3650 cm^{-1} are associated with the stretching vibration of hydroxyl (−OH) group from intermolecular and intramolecular hydrogen bonds (region I in Figure 4) and their intensity were observed relatively decreasing when compared to neat as-electrospun PVA nanofibrous mat as the vapor cross-linking time increases indicating that more of the −OH groups are involved in the formation of acetal bridge. The two vibrational bands observed between 2730 and 2860 cm^{-1} refer to the stretching vibration of C−H from alkyl and O═C−H from the aldehyde (region II in Figure 4) and the bands between 1700 and 1750 cm^{-1} (region III in Figure 4) are due to the C═O stretching of the unreacted end of the aldehyde[14,43] in the vapor cross-linked PVA nanofibrous mat. The band observed at 1000−1140 cm^{-1} with gradual broadening of the peak width as the cross-linking reaction time increase is attributed to O−C−O vibration of the acetal group[43] (see region IV in Figure 4).

Once the presence of free aldehyde groups were demonstrated by FTIR on the surface of GA vapor cross-linked PVA nanofibrous mats, the content of the free aldehyde groups were then determined by using tyramine/BCA assay where the hydroxyphenyl functional group of tyramine as labeling group for free aldehyde groups. Thus, the 2.0 M GA vapor cross-linked PVA mat contains 2.16 $nmol/mm^2$ free unreacted aldehyde groups while 2.56 M GA vapor cross-linked one contains 2.24 $nmol/mm^2$. The free aldehyde groups on the nanofibrous mat cross-linked by lower GA vapor concentrations were hardly detected by FTIR (see the Supporting Information, Figure S3).

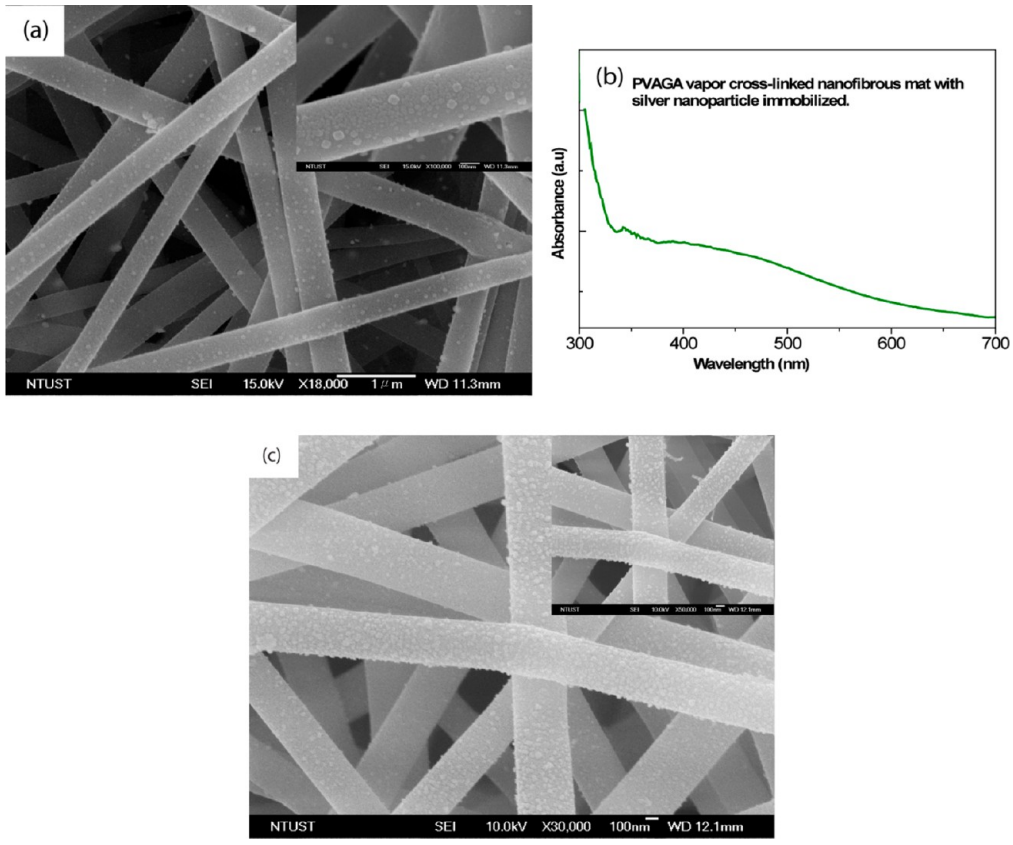

Figure 6. (a) SEM micrograph of Ag nanoparticles immobilized/reduced by aldehyde on the surface of vapor cross-linked PVA nanofibrous mat (inset: at higher magnification of the fiber, scale bar 100 nm), (b) UV−visible absorption spectrum of the fibrous mat containing Ag, (c) surfaces of GA vapor cross-linked PVA nanofibers covered by Ag nanoparticle formed by Tollen's reagent (ammoniacal $AgNO_3$) (inset: 50 000× magnification, scale bar 100 nm).

In Situ Formation of Silver Nanoparticles. The vapor phase cross-linked nanofibrous mat was tested for its water resistance by soaking it in water for 6, 12, 24, and 48 h. Interestingly, all the vapor phase cross-linked nanofibrous mats with GA vapor exposure concentrations of 0.5 to 2.56 M were found to be stable and their fiber morphology remained intact as it was in the vapor cross-linking (see Figure 5a and b, and for more SEM images, see the Supporting Information, Figure S4). The significance of our approach offers other flexible benefits in addition to rendering PVA nanofibrous mat water insoluble. The vapor phase cross-linked PVA nanofibrous mat contains one end of the GA unreacted to the hydroxyl group of the PVA (see Scheme 1a). Immersing the cross-linked PVA nanofibrous mat in aqueous silver nitrate ($AgNO_3$) solution resulted in an in situ reduction of silver (Ag) ion by the unreacted end of the GA at room temperature. A similar experiment using Tollen's reagent (ammoniacal $AgNO_3$ solution) was carried out to observe the effectiveness of aldehyde groups in the cross-linked nanofibrous mat on reducing silver ions to silver nanoparticles. Evidently, Ag nanoparticles can be generated in situ by the free aldehyde groups in the cross-linked PVA nanofibrous mat (Figure 6). The reaction equation/mechanism for ammoniacal $AgNO_3$, as shown in Scheme 1b, involved the free aldehyde in the cross-linked fibers acting as a reducing agent and subsequently oxidized into carboxylate while silver ions reduced and deposited onto the surfaces of the individual cross-linked nanofibers.

Figure 6a showed that the surfaces of the cross-linked PVA nanofibers were significantly covered with Ag nanoparticles with average size of 20−46 nm in situ reduce by the aldehyde in aqueous $AgNO_3$ solution possibly by analogous mechanism where the aldehyde acted as a reducing agent and donate electrons and thereby oxidized into carboxylate with concomitant reduction of the silver ions by accepting electrons into silver nanoparticles. The SEM micrograph shown in Figure 6c illustrated the surfaces of the GA vapor cross-linked PVA nanofibers decorated with silver nanoparticles immersed in ammoniacal $AgNO_3$. Further evidence for the reduction and existence of Ag was confirmed by EDX analysis with weight percentage of C = 62.81, O = 29.04, and Ag = 8.15. The absorption band centered at about 400 nm, occurring due to collective excitation of free electrons of Ag nanoparticles in resonance with the light wave[39] in the UV−vis absorption, was complementary evidence for the in situ reduction of silver by aldehyde (see Figure 6b). The content of silver nanoparticles present in nanofibrous mat was determined by ICP-AES to be 4.60 and 5.76% in 2.0 and 2.56 M GA cross-linked mat, respectively which in turn also agreed with the content of unreacted aldehyde groups present in each GA vapor cross-linked PVA mats which were 2.16 nmol/mm^2 (in 2.0 M) and 2.24 nmol/mm^2 (in 2.56 M). This again indicates the advantage of employing a higher GA concentration for vapor phase cross-linking PVA; it not only can well preserve the original morphology of the as-spun nanofibers but also provides more unreacted aldehyde groups for the in situ formation of more Ag nanoparticles.

Antimicrobial Activity of the Ag Nanoparticles-Immobilized Nanofibrous Mat. PVA nanofibrous mat with

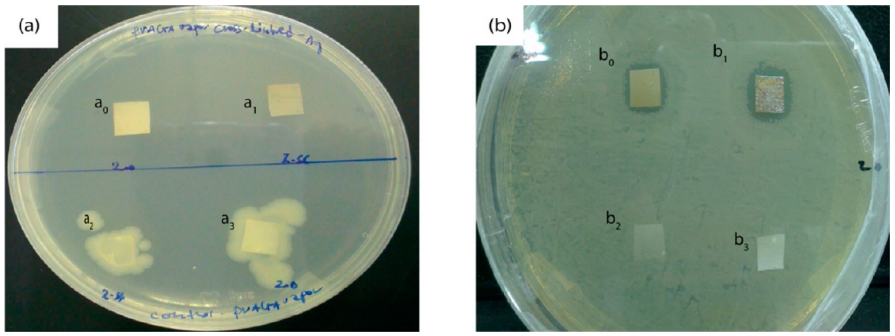

Figure 7. Antimicrobial activity of Ag nanoparticle immobilized nanofibrous mat (a) a_0, a_1 are nanofibrous mat containing Ag nanoparticle and sprayed with *E. coli* bacteria (OD_{600} = 0.05), and a_2, a_3 are control group only vapor cross-linked PVA mats and sprayed with *E. coli* bacteria (OD_{600} = 0.05), (b) b_0, b_1 are the clear inhibition zone test of Ag immobilized nanofibrous mat against *E. coli* and b_2, b_3 are control groups without Ag.

in situ formed Ag nanoparticles was tested for its potential antimicrobial activity against *E. coli*. As shown by inhibition zone test on LB agar plate (Figure 7), a clear circular zone of inhibition (19.3 mm of the final inhibition zone diameter for both 2.56 M GA (initial length of the square mat 13.7 mm) and 2.0 M GA (initial length 12.6 mm)) was observed because of the slow released Ag ions and diffuses out of the fibrous mat and kills and inhibits the growth of the *E. coli* in a certain diameter outward (see Figure 7b_0, b_1). However, for the control (only GA vapor cross-linked PVA nanofibrous mat) there was no clear zone of inhibition (see Figure 7b_2, b_3). In addition to the inhibition zone test, the antimicrobial activity of Ag nanoparticles immobilized nanofibrous mat was also tested by spraying bacterial suspension (OD_{600} = 0.05) onto nanofibrous mats and checking the survival rate of bacteria by laying the mats on LB agar plate. As shown in Figure 7a_2, a_3, large bacteria colonies were observed around the edges of the fibrous mat for the control and there were no colonies growing around the Ag nanoparticles immobilized nanofibrous mat (Figure 7a_0, a_1). Evidently, the bacteria sprayed onto the control mat can survive and spread outward from the mat. In contrast, the bacteria sprayed on the Ag nanoparticles immobilized nanofibrous mat were captured by the fine nanofibrous structure and effectively killed by the Ag ions released from Ag nanoparticles, which leads to the very clean edges observed on LB agar plate.

CONCLUSIONS

The study demonstrated that the as-electrospun PVA nanofibrous mat, which is instantly water-soluble, can be effectively cross-linked by exposing it to vapor phase GA and render it water-insoluble. In addition to making it water-resistant, the GA vapor cross-linked fibrous mat found to contain unreacted end of the GA, which is a potential reaction site for reduction of Ag ion. We successfully demonstrated the reduction of $AgNO_3$ aqueous solution in to Ag nanoparticle at ambient temperature by the unreacted end of GA in the cross-linked PVA nanofibrous mat without the addition of any reducing or toxic agents and which makes the method greener and environmentally friendly. Consequently, this PVA nanofibrous mat with in situ formed Ag nanoparticles demonstrates its potent antimicrobial activity against *E. coli*.

Therefore, the result of our work showed that the unreacted GA on the vapor cross-linked nanofibrous mat could be used as a potential reduction and immobilization matrix of high specific surface area not only for silver but also other metal nanoparticles. Hence, the nanofibrous mat with in situ reduced silver nanoparticles produced in such approach can be used in applications such as antimicrobial agent, wound dressing, water or air purification, as SERS substrate, and in catalysis.

ASSOCIATED CONTENT

Supporting Information

SEM images of the vapor cross-linked PVA nanofibrous mat for different vapor exposure time, digital images of neat as-electrospun PVA and vapor cross-linked PVA nanofibrous mat soaked in water, FTIR spectra for different concentration of vapor exposures. This material is available free of charge via the Internet at http://pubs.acs.org.

AUTHOR INFORMATION

Corresponding Author

*E-mail: cklee@mail.ntust.edu.tw. Tel:+886-227376629. Fax: +886-227376644.

Notes

The authors declare no competing financial interest.

ACKNOWLEDGMENTS

The authors thank Taiwan Building Technology Center for funding and Mr. Sheng Chang Laiw for his assistance in SEM. A.G. is greatly indebted to National Taiwan University of Science and Technology, Department of Chemical Engineering, for a graduate study scholarship grant.

REFERENCES

(1) Supaphol, P.; Chuangchote, S. *J. Appl. Polym. Sci.* **2008**, *108*, 969−978.
(2) Wong, K. K. H.; Hutter, J. L.; Zinke-Allmang, M.; Wan, W. *Eur. Polym. J.* **2009**, *45*, 1349−1358.
(3) Huang, Z.-M.; Zhang, Y. Z.; Kotaki, M.; Ramakrishna, S. *Compos. Sci. Technol.* **2003**, *63*, 2223−2253.
(4) Han, D.; Filocamo, S.; Kirby, R.; Steckl, A. J. *ACS Appl. Mater. Interfaces* **2011**, *3*, 4633−4639.
(5) Miao, Y.-E.; Wang, R.; Chen, D.; Liu, Z.; Liu, T. *ACS Appl. Mater. Interfaces* **2012**, *4*, 5353−5359.
(6) Teo, W. E.; Ramakrishna, S. *Nanotechnology* **2006**, *17*, R89−R106.
(7) Ding, B.; Kim, H.-Y.; Lee, S.-C.; Shao, C.-L.; Lee, D.-R.; Park, S.-J.; Kwag, G.-B.; Choi, K.-J. *J. Polym. Sci., Part B: Polym. Phys.* **2002**, *40*, 1261−1268.
(8) Hang, A. T.; Tae, B.; Park, J. S. *Carbohydr. Polym.* **2010**, *82*, 472−479.
(9) Wang, X.; Chen, X.; Yoon, K.; Fang, D.; Hsiao, B. S.; Chu, B. *Environ. Sci. Technol.* **2005**, *39*, 7684−7691.
(10) Wang, J.; Yao, H.-B.; He, D.; Zhang, C.-L.; Yu, S.-H. *ACS Appl. Mater. Interfaces* **2012**, *4*, 1963−1971.

(11) Taepaiboon, P.; Rungsardthong, U.; Supaphol, P. *Nanotechnology* **2006**, *17*, 2317−2329.
(12) Koski, A.; Yim, K.; Shivkumar, S. *Mater. Lett.* **2004**, *58*, 493−497.
(13) Zhang, C.; Yuan, X.; Wu, L.; Han, Y.; Sheng, J. *Eur. Polym. J.* **2005**, *41*, 423−432.
(14) Jia, Y.-T.; Gong, J.; Gu, X.-H.; Kim, H.-Y.; Dong, J.; Shen, X.-Y. *Carbohydr. Polym.* **2007**, *67*, 403−409.
(15) Hong, K. H. *Polym. Eng. Sci.* **2007**, *47*, 43−49.
(16) Taepaiboon, P.; Rungsardthong, U.; Supaphol, P. *Nanotechnology* **2007**, *18*, 175102.
(17) Reneker, D. H.; Chun, I. *Nanotechnology* **1996**, *7*, 216.
(18) Doshi, J.; Reneker, D. H. *J. Electrostat.* **1995**, *35*, 151−160.
(19) Zeng, J.; Xu, X.; Chen, X.; Liang, Q.; Bian, X.; Yang, L.; Jing, X. *J. Controlled Release* **2003**, *92*, 227−231.
(20) Yao, L.; Haas, T. W.; Guiseppi-Elie, A.; Bowlin, G. L.; Simpson, D. G.; Wnek, G. E. *Chem. Mater.* **2003**, *15*, 1860−1864.
(21) Kumar, J.; D'Souza, S. F. *Talanta* **2008**, *75*, 183−188.
(22) Praptowidodo, V. S. *J. Mol. Struct.* **2005**, *739*, 207−212.
(23) Tang, C.; Saquing, C. D.; Harding, J. R.; Khan, S. A. *Macromolecules* **2010**, *43*, 630−637.
(24) Wang, Y.; Hsieh, Y.-L. *J. Appl. Polym. Sci.* **2010**, *116*, 3249−3255.
(25) Bolto, B.; Tran, T.; Hoang, M.; Xie, Z. *Prog. Polym. Sci.* **2009**, *34*, 969−981.
(26) Ramires, P. A.; Milella, E. *J. Mater. Sci.: Mater. Med.* **2002**, *13*, 119−123.
(27) Wu, L.; Yuan, X.; Sheng, J. *J. Membr. Sci.* **2005**, *250*, 167−173.
(28) Yang, D.-J.; Kamienchick, I.; Youn, D. Y.; Rothschild, A.; Kim, I.-D. *Adv. Funct. Mater.* **2010**, *20*, 4258−4264.
(29) Signori, A. M.; Santos, K. d. O.; Eising, R.; Albuquerque, B. L.; Giacomelli, F. C.; Domingos, J. B. *Langmuir* **2010**, *26*, 17772−17779.
(30) Zhang, L.; Gong, X.; Bao, Y.; Zhao, Y.; Xi, M.; Jiang, C.; Fong, H. *Langmuir* **2012**, *28*, 14433−14440.
(31) He, D.; Hu, B.; Yao, Q.-F.; Wang, K.; Yu, S.-H. *ACS Nano* **2009**, *3*, 3993−4002.
(32) Rujitanaroj, P.-o.; Pimpha, N.; Supaphol, P. *Polymer* **2008**, *49*, 4723−4732.
(33) Xiao, S.; Shen, M.; Guo, R.; Wang, S.; Shi, X. *J. Phys. Chem. C* **2009**, *113*, 18062−18068.
(34) Bagihalli, G. B.; Avaji, P. G.; Patil, S. A.; Badami, P. S. *Eur. J. Med. Chem.* **2008**, *43*, 2639−2649.
(35) Zhang, Y.; Peng, H.; Huang, W.; Zhou, Y.; Yan, D. *J. Colloid Interface Sci.* **2008**, *325*, 371−376.
(36) Ghule, K.; Ghule, A. V.; Chen, B.-J.; Ling, Y.-C. *Green Chem.* **2006**, *8*, 1034−1041.
(37) Heinlaan, M.; Ivask, A.; Blinova, I.; Dubourguier, H.-C.; Kahru, A. *Chemosphere* **2008**, *71*, 1308−1316.
(38) Liao, Y.; Wang, Y.; Feng, X.; Wang, W.; Xu, F.; Zhang, L. *Mater. Chem. Phys.* **2010**, *121*, 534−540.
(39) Sureshkumar, M.; Siswanto, D. Y.; Lee, C.-K. *J. Mater. Chem.* **2010**, *20*, 6948−6955.
(40) Deng, Z.; Zhu, H.; Peng, B.; Chen, H.; Sun, Y.; Gang, X.; Jin, P.; Wang, J. *ACS Appl. Mater. Interfaces* **2012**, *4*, 5625−5632.
(41) Kumar, A.; Vemula, P. K.; Ajayan, P. M.; John, G. *Nat. Mater.* **2008**, *7*, 236−241.
(42) Dallas, P.; Tucek, J.; Jancik, D.; Kolar, M.; Panacek, A.; Zboril, R. *Adv. Funct. Mater.* **2010**, *20*, 2347−2354.
(43) Mansur, H. S.; Sadahira, C. M.; Souza, A. N.; Mansur, A. A. P. *Mater. Sci. Eng., C* **2008**, *28*, 539−548.
(44) Hong, K. H.; Park, J. L.; Sul, I. H.; Youk, J. H.; Kang, T. J. *J. Polym. Sci., Part B: Polym. Phys.* **2006**, *44*, 2468−2474.
(45) Ghasemi, M.; Minier, M.; Tatoulian, M.; Arefi-Khonsari, F. *Langmuir* **2007**, *23*, 11554−11561.
(46) Fang, X.; Ma, H.; Xiao, S.; Shen, M.; Guo, R.; Cao, X.; Shi, X. *J. Mater. Chem.* **2011**, *21*, 4493−4501.
(47) Choi, S. S.; Lee, S. G.; Joo, C. W.; Im, S. S.; Kim, S. H. *J. Mater. Sci.* **2004**, *39*, 1511−1513.